SUDDEN SHORT-CIRCUIT CURRENT OF INDUCTOR ALTERNATORS

By

P. Asztalos

Department of Electrical Machines, Polytechnical University, Budapest

(Received March 31, 1964)

1. Introduction

Many publications have appeared on theoretical aspects of inductor-alternators. Among these, however, only a single paper makes reference to

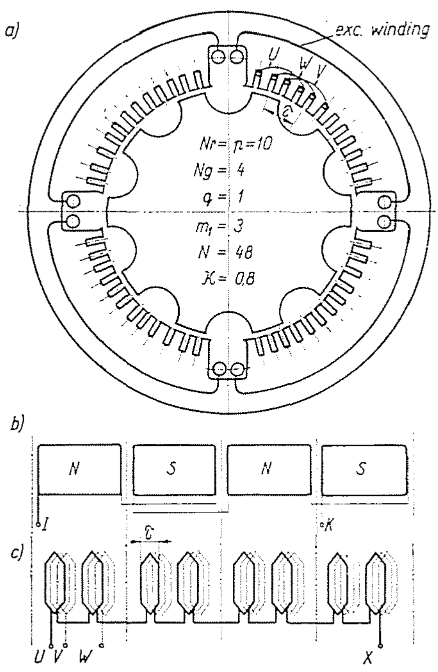

Fig. 1. Three-phase inductor alternators
a) cross-sectional view
b) development diagram of field-winding
c) development diagram of armature winding

the transient behaviour of the specially built synchronous machines [1]. The author of this paper, Alper states that — owing to the greater difference existing between the air-gap field of excitation and armature windings — the transient and synchronous reactances of inductor-alternators differ from each other less than in the case of normal alternate-pole synchronous alternators.

The said paper published no numerical data and also fails to investigate to what extent the harmonics of air-gap field and the leakage reactances of both windings influence the transient behaviour of these machines. No mention is made in it of subtransient reactance, either.

In the following, an attempt is made to clarify these problems in a qualitative way.

Investigation of flux-linkages and transient phenomena will be carried out for a *three-phase heteropolar inductor-alternator.*

Let it be assumed that the *magnetic circuit* is *laminated* throughout, the machine has no damper windings and magnetic permeability of the iron-core is being considered as infinite.

Cross-sectional view and winding development diagram of a three-phase heteropolar alternator is shown in Fig. 1. In the case being illustrated, the stator has four excitation poles. Between the spacious slots of the excitation winding are located the smaller slots of the three-phase armature-winding.

2. Harmonic components of air-gap field. Flux linkages between the two windings

Permeance of the air-gap in inductor machines, *at synchronous speed,* related to the coordinate system fixed to the stator [1]

$$p(a, t) = p_0 + p_1 \cdot \cos(a - \omega t) + p_2 \cdot \cos(2a - 2\,\omega t) + \dots \qquad (2.1)$$

As shown by Doherty and Nickle [4], the air-gap permeance harmonics assume different values dependent on which harmonics of the stator m. m. f. they are related to [1].

Nevertheless, since in our investigations the *fundamental* of the armature m. m. f. is only taken into consideration, the specific permeance-harmonics obtainable from flux-distribution diagrams will be regarded in the following as having constant value. As to their determination, the flux-distribution diagrams plotted for *constant* circumferential m. m. f. serve.

In the following let us investigate which flux-density waves exist in the air-gap of a three-phase inductor-machine when at synchronous speed, if in the armature windings a symmetrical three-phase a. c. of fundamental frequency is flowing. Fundamental harmonic of the rotating m. m. f. produced by stator-current is

$$\Theta_{a1} = \Theta_{a1\max} \cdot \cos(a - \omega t) \qquad (2.2)$$

2.1 *Air-gap fields of direct axis at synchronous speed*

Flux-density waves created by the fundamental harmonic of stator m. m. f. at synchronous speed can be calculated from Equations (2.1) and (2.2) in the case when the rotor teeth are permanently facing the fundamental wave of the rotating m. m. f. of the stator. This condition corresponds to *direct axis position* of a normal synchronous machine [1]. When short-circuited, this is the very relative position of rotor and armature m. m. f.-s. In this case

$$\Theta_{a1\max}\left[\left(p_0+\frac{p_2}{2}\right)\cdot\cos(a-\omega t)+\frac{p_1}{2}+\frac{p_1+p_3}{2}\cdot\cos(2a-2\omega t)+\dots\right] \quad (2.3)$$

flux-density waves are present in the air-gap. The first term represents the fundamental field rotating synchronously with the rotor and inducing e. m. f. of fundamental frequency in the armature windings. This corresponds to *direct armature reaction* [1, 4] of a salient-pole machine, but is not linked with the excitation windings. Neither this term, nor any other term representing

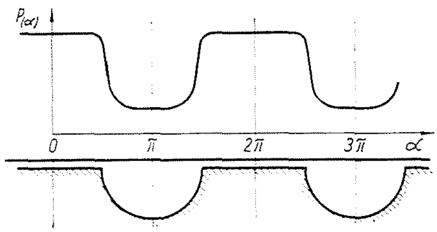

Fig. 2. Specific air-gap magnetic permeance in an inductor machine

rotating fields produce e. m. f. in the excitation windings. The remaining terms of field produce harmonic e. m. f.-s in the armature. The second term, however, represents a field stationary in space and unvarying in time too, having contrary sign under contiguous poles and thus representing a flux linked constantly and positively with the excitation windings and corresponding to *mutual inductance* of the two windings.

2.2 *Air-gap fields of quadrature axis at synchronous speed*

If the rotor teeth lay permanently at right angles (in magnetic sense) to the axis of stator m. m. f. that is, at quadrature axis, in the air-gap the following flux-density waves are established

$$\Theta_{a1\max}\cdot\left[\left(p_0-\frac{p_2}{2}\right)\cdot\sin(a-\omega t)+\frac{p_1-p_3}{2}\cdot\sin(2a-2\omega t)+\dots\right] \quad (2.4)$$

It can be seen that *at quadrature axis no stationary field exists*, consequently, in this case *no flux-linkage* is present between the two windings [1]. The first term represents a field rotating synchronously with the rotor and inducing e. m. f. of fundamental frequency in armature. This corresponds with *quadrature armature reaction* [4] of salient pole machines. The rest of the terms are producing harmonics in the armature. Again, in the excitation winding neither of them can induce an e. m. f.

3. Air-gap fields at no-load and in short-circuit

At no-load the excitation winding provides a constant m. m. f. $\Theta_{gü}$ and as a result of this, the flux-density waves

$$\Theta_{gü} \cdot [p_0 + p_1 \cdot \cos(a - \omega t) + p_2 \cdot \cos(2\,a - 2\omega t) + \ldots] \tag{3.1}$$

are produced in the air-gap. Out of these the permanent field $p_0 \cdot \Theta_{gü}$ is to be linked with the excitation winding, in the armature windings the rotating field $p_1 \cdot \Theta_{gü} \cdot \cos(a - \omega t)$ produces fundamental e. m. f. while the other fields (of odd order) induce harmonic e. m. f.

In short-circuit, the resultant air-gap field can be calculated from formulae (2.3) and (3.1), considering that Θ_g and Θ_a have contrary effects

$$\left[\Theta_g \cdot p_0 - \Theta_{a1\max} \cdot \frac{p_1}{2}\right] + \left[\Theta_g \cdot p_1 - \Theta_{a1\max} \cdot \left(p_0 + \frac{p_2}{2}\right)\right] \cdot \cos(a - \omega t) +$$

$$+ \left[\Theta_g \cdot p_2 - \Theta_{a1\max} \cdot \frac{p_1 + p_3}{2}\right] \cdot \cos(2a - 2\omega t) + \ldots \tag{3.2}$$

It can be seen that in inductor machines the field $\left[\Theta_g \cdot p_0 - \Theta_{a1\max} \cdot \frac{p_1}{2}\right]$ is constantly linked with the excitation winding, while the term

$$\left[\Theta_g \cdot p_1 - \Theta_{a1\max} \cdot \left(p_0 + \frac{p_2}{2}\right)\right] \cdot \cos(a - \omega t) \tag{3.3}$$

induces the fundamental e. m. f. required for covering the voltage drop produced by armature leakage reactance.

4. Short-circuit characteristic

Neglecting the resistance of armature winding by use of expression (3.3) it can be written that

$$c \cdot I_a \cdot X_{s1} = \Theta_{a1\max} \cdot p_{s1} = \Theta_g \cdot p_1 - \Theta_{a1\max} \cdot \left(p_0 + \frac{p_2}{2}\right) \tag{4.1}$$

ince for description of air-gap fields the magnetic permea nces of the various harmonics have previously been made use of, it will also be convenient instead of the leakage reactance to calculate with its equivalent permeance p_{s1}:

$$p_{s1} = \frac{\pi^2 \cdot \sum \frac{\lambda}{q}}{3 \cdot \xi_1^2 \cdot \tau} \tag{4.2}$$

From Equation (4.1)

$$\Theta_{a1\max} = \Theta_g \cdot \frac{p_1}{p_0 + \frac{p_2}{2} + p_{s1}} \tag{4.3}$$

In the case of a three-phase stator, taking also the number of slots necessarily omitted for excitation slots into consideration, the amplitude of armature m. m. f. fundamental can be given as

$$\Theta_{a1\max} = \frac{3 \cdot \sqrt{2} \cdot w \cdot \xi_1 \cdot I_a}{\pi \cdot \varkappa \cdot p} \tag{4.4}$$

Omission of slots was considered by the factor

$$\varkappa = \frac{N}{2 \cdot q \cdot p} \tag{4.5}$$

5. Initial short-circuit current

Let us examine what initial current arises when simultaneously shorting a three-phase inductor alternator without damper, in all phases.

To this end, the train of thought [8] usual for the determination of initial currents in conventional alternate-pole machines can be followed.

For a start, this time, too, we may resort to the *constant linkage theorem*. According to our method of discussion hitherto adopted we will reckon, however, instead of currents I with the corresponding m. m. f.-s Θ and, instead of inductances L with the magnetic permeances p proportional to them.

The stator terminals of the alternator would be shorted from no-load at the very instant the rotor teeth were exactly in line with the magnetic axis of one of the phase-windings. At the moment of short-circuit, according to Equation (3.1) the flux

$$\Psi_a = c \cdot \Theta_{g\ddot{u}} \cdot p_1 \tag{5.1}$$

has been linked to the selected phase-winding.

At the same time, by (3.1) the flux

$$\Psi_g = c \cdot \Theta_{g\ddot{u}} \cdot (p_0 + p_{s2}) \tag{5.2}$$

was linked to field winding; here p_{s2} is the specific leakage permeance of field winding.

When the short-circuit is completed, the flux linked to armature winding will be the sum of fluxes produced by armature currents and excitation currents. Resultant flux-linkages are the same as the fluxes linked to the windings before shorting. On the basis of Equation (3.3)

$$\left.\begin{aligned} \Psi_a &= -(\Theta_{av}+\Theta_{ae})\cdot\left(p_0+\frac{p_2}{2}+p_{s1}\right)+(\Theta_{gv}+\Theta_{ge})\cdot p_1=\Theta_{g\ddot{u}}\cdot p_1 \\ \Psi_g &= -(\Theta_{av}+\Theta_{ae})\cdot\frac{p_1}{2}+(\Theta_{gv}+\Theta_{ge})\cdot(p_0+p_{s2})=\Theta_{g\ddot{u}}\cdot(p_0+p_{s2} \end{aligned}\right\} \tag{5.3}$$

After transforming and arranging these equations, we obtain

$$\Theta_{av}=-\Theta_{ae} \tag{5.4}$$

It can be seen that, similarly to alternate-pole machines, *a d. c. component is present in the short-circuit current of inductor machines, too.*

Now, let us examine the flux-linkages in the rotor position occupied after a quarter period.

A. c. m. m. f. Θ_{av} having rotated together with the rotor as well, direct current m. m. f. Θ_{ae} remained stationary. D. c. m. m. f. Θ_{ge} of the field winding has not altered, while a. c. m. m. f. Θ_{gv} has decreased within the quarter period from its highest initial value to zero.

As in the direction perpendicular to the selected armature phase winding, at the moment of short-circuit no flux had been linked to the armature, in this direction also the flux-linkage becomes zero after shorting

$$\Psi_a=-\Theta_{av}\cdot\left(p_0+\frac{p_2}{2}+p_{s1}\right)+\Theta_{ge}\cdot p_1=0$$

and the flux linked to field winding (5.5)

$$\Psi_g=-\Theta_{av}\cdot\frac{p_1}{2}+\Theta_{ge}\cdot(p_0+p_{s2})=\Theta_{g\ddot{u}}\cdot(p_0+p_{s2})$$

After arranging

$$\Theta_{av}=\Theta_{g\ddot{u}}\cdot\frac{p_1}{\left(p_0+\frac{p_2}{2}+p_{s1}\right)-\frac{p_1^2}{2\cdot(p_0+p_{s2})}} \tag{5.6}$$

The quotient of equations (5.6) and (4.3) gives the proportion of the synchronous (X_d) and transient (X_d') reactances:

$$\frac{X_d}{X_d'}=\frac{p_0+\frac{p_2}{2}+p_{s1}}{p_0+\frac{p_2}{2}+p_{s1}-\frac{p_1^2}{2\cdot(p_0+p_{s2})}} \tag{5.7}$$

6. Synchronous and transient reactance

Equation (5.7) obtained for an inductor machine lends itself for comparison with the discussions of Alper [1], these being of general nature. According to his cited paper, for inductor alternators

$$X_d' = X_{s1} + \cfrac{1}{\cfrac{1}{X_{ad}\cdot(k-1) + X_{s2}'\cdot\cfrac{X_{ad}}{X_g}\cdot k} + \cfrac{1}{X_{ad}}} \tag{6.1}$$

where

$$k = \frac{X_{ad}\cdot X_g}{X_m^2} \tag{6.2}$$

Alper gives no physical explanation for the interpretation of reactance X_m of mutual inductance and for that of field-winding air-gap flux reactance X_g. The explanation appears from the results obtained in Para. 5 of the present paper.

Namely, with Equations (6.1) and (6.2)

$$\frac{X_d}{X_d'} = \frac{X_{s1} + X_{ad}}{X_{s1} + X_{ad} - \cfrac{X_m^2}{X_g + X_{s2}'}} \tag{6.3}$$

By comparing the equations (6.3) and (5.7) it becomes evident that between the various reactances and air-gap permeance harmonics on the one hand, and the reactances and leakage permeances on the other hand, the following relations exist

$$\left.\begin{aligned} X_{ad} &= C\cdot\left(p_0 + \frac{p_2}{2}\right), & X_{aq} &= C\cdot\left(p_0 - \frac{p_2}{2}\right) \\ X_g &= C\cdot p_0, & X_m &= C\cdot\frac{p_1}{\sqrt{2}} \\ X_{s1} &= C\cdot p_{s1}, & X_{s2}' &= C\cdot p_{s2} \end{aligned}\right\} \tag{6.4}$$

where

$$C = \frac{12\cdot\tau\cdot w^2\cdot f\cdot \xi_1^2\cdot l_i\cdot 10^{-8}}{\pi\cdot p\cdot \varkappa} \tag{6.5}$$

and from Equations (6.2) and (6.4)

$$k = \frac{\left(p_0 + \cfrac{p_2}{2}\right)\cdot p_0}{p_1^2}\cdot 2 \tag{6.6}$$

As Alper [1] pointed out, the factor k is of higher value for inductor machines than for alternate-pole machines and, therefore, the difference between synchronous and transient reactances is less with the former. Also, its value can be calculated from air-gap permeance harmonics by means of relation (6.6). From Fig 10 it can be seen that $k > 1$.

In practical cases

$$0,3 < z/t < 0,5 \tag{6.7}$$

and

$$\delta/t > 0,015 \tag{6.8}$$

and, consequently, for inductor machines generally

$$k \geqq 1,5 \tag{6.9}$$

while for alternate-pole machines $k \approx 1$.

This difference alone accounts for the fact that for the former machines the ratio X_d/X_d' is lower. In addition, *the leakage of windings is much larger* on inductor machines than on alternate-pole machines. As can be demonstrated, i.e., the usual leakage permeances are in the former case

$$\frac{p_{s1}}{p_0 + \frac{p_2}{2}} \geqq 0,2 \quad \text{and} \quad \frac{p_{s2}}{p_0 + \frac{p_2}{2}} \geqq 1,2 \tag{6.10}$$

as compared with that of alternate-pole machines

$$p_{s1} \cong p_{s2} \cong \frac{p_0 + \frac{p_2}{2}}{10} \tag{6.10a}$$

By replacing these values into Equation (5.7), we obtain approximately

$$\frac{X_d}{X_d'} \leqq 1,3 \tag{6.11}$$

By contrast, for alternate-pole machines $X_d/X_d' = 3$ to 10.

It is because of *multipole layout* ($2p = 20 \sim 50$) that the leakage reactance of stator winding ($X_{s1} = C \cdot p_{s1}$) grows as compared with armature reaction X_{ad}. The field winding leakage reactance *(X_{s2}')* is much greater here than with normal alternate-pole machines because here the *number of excitation slots* is generally only *a fraction of that of armature slots.*

Consequently, *the initial short-circuit current of three-phase inductor alternators without dampers will always be much less than that of alternate-pole machines*, and it can be at most

$$1,8 \cdot \sqrt{2} \cdot \frac{X_d}{X_d'} = 1,8 \sqrt{2} \cdot 1,3 = 3,3 \tag{6.12}$$

This maximum initial current is encountered in alternators of the frequency order of about 500 cps where the number of poles is relatively low, and thus the rotor tooth pitch ($t = 2\tau$) relatively large. For lower frequencies than this, inductor alternators are usually not built. For machines of higher frequencies the value of δ/t will be higher, too, and the initial current less than given by (6.12).

Equations (5.3) show that, theoretically, the excitation current contains transient components as well as in alternate-pole machines.

Owing to low initial armature current and loose flux linkage, however, when simultaneously shorting an inductor machine in all three phases, as a rule, *in the field current scarcely any transient phenomena can be observed.*

7. Subtransient reactance

In the foregoing, a three-phase heteropolar inductor alternator having no damper circuits whatever has been examined. However, in many cases

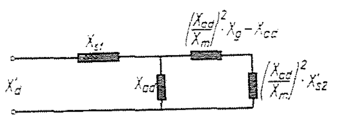

Fig. 3. Equivalent circuit of transient reactance X'_d

short-circuited *damping turns* are employed, which are concentrically laid out with the field-windings of the alternator. Their existence can be considered by replacing them with a winding connected parallel to field winding.

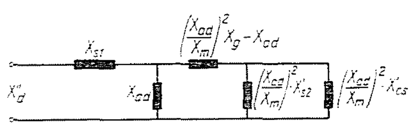

Fig. 4. Equivalent circuit of subtransient reactance X''_d

According to Equation (6.3), for the direct axis *transient reactance* an equivalent circuit diagram can be drawn, as in the case of alternate-pole machines. The scheme first published in the literature by ALPER [1] is shown in a slightly modified form in Fig 3.

The equivalent circuit diagram of direct axis *subtransient reactance* can be obtained by connecting in Fig 3 the reactance $\left(\dfrac{X_{ad}}{X_m}\right)^2 \cdot X'_{cs}$ corresponding to leakage reactance X'_{cs} of damper turns reduced to armature winding, parallel to reactance $\left(\dfrac{X_{ad}}{X_m}\right)^2 \cdot X'_{s2}$, see Fig 4. From this diagram the direct axis substransient reactance can also be expressed as

$$X_d'' = X_{s1} + X_{ad} - \frac{X_m^2}{X_g + \dfrac{X_{cs}' \cdot X_{s2}'}{X_{cs}' + X_{s2}'}} \tag{7.1}$$

Similar to Equation (6.11) let us examine the value of quotient X_d/X_d'' characteristic of the subtransient initial current of inductor machines.

In extreme cases, when $X_{cs}' \ll X_{s2}'$ or $X_{cs}' \cong 0$, respectively, that is for short-circuited windings having *a perfect damping effect*

$$X_d'' = X_{s1} + X_{ad} - \frac{X_m^2}{X_g} = X_d - \frac{X_{ad}}{k} \tag{7.2}$$

The corresponding equivalent circuit diagram is shown on Fig 5. It is in this case that the maximum possible initial current arises.

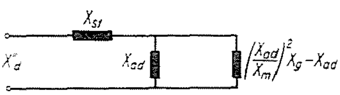

Fig. 5. Equivalent circuit of subtransient reactance X_d'' if $X_{cs}' = 0$

The corresponding reactance ratio will be

$$\frac{X_d}{X_d''} = \frac{p_0 + \dfrac{p_2}{2} + p_{s1}}{p_0 + \dfrac{p_2}{2} + p_{s1} - \dfrac{p_1^2}{2 \cdot p_0}} \tag{7.3}$$

For extremities according to (6.7), (6.8) and (6.10)

$$\frac{X_d}{X_d''} \leq 2{,}36 \tag{7.4}$$

Comparing (7.4) with (6.11) it can be seen that in case of perfect damping the substransient a.c. may by 80 per cent exceed the transient a.c. of a machine having no damper winding, but even in this extreme case it will be much less than the subtransient short-circuit a.c. of an alternate-pole machine.

The damper turns are located at the bottom of the excitation slot or under its wedges. Also, there is another arrangement in which the damping turns are wound onto the stator core (Fig 6). The most satisfactory damper is that one arranged under the wedges, this in fact having a leakage reactance much less than that of the field winding lying under it. For reasons of manufacture, however, this latter layout is often unpractical.

With *damping turns arranged at the slot bottom*, X'_{cs} is of the same order as X'_{s2} and in this case

$$X''_d \cong X_{s1} + X_{ad} - \frac{X_m^2}{X_g + \frac{X'_{s2}}{2}} \cong C \cdot \left[p_{s1} + p_0 + \frac{p_2}{2} - \frac{p_1^2}{2 \cdot \left(p_0 + \frac{p_{s2}}{2} \right)} \right] \quad (7.5)$$

Again, in the most unfavourable cases characterised by (6.7), (6.8) and (6.10) the reactance ratio will be about

$$\frac{X_d}{X''_d} \leq 1{,}44 \quad (7.6)$$

Thus, for dampers arranged at the slot bottom, the subtransient reactance can only be by about 10 per cent less than the transient reactance.

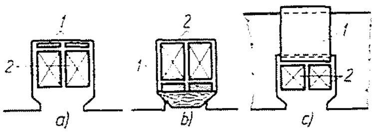

Fig. 6. Arrangement of damping turns in heteropolar machines
a) at slot bottom
b) under slot wedge
c) around core
1. damping turn
2. field-winding

It should be stressed that the reactance ratios given by Equations (6.11), (7.4) and (7.8) are extreme values which are valid for the most unfavourable tooth-shapes encountered in practice, that is, for 500 cps. On middle-frequency alternators of several thousand cps, where $\delta/t > 0{,}015$ and thus, according to Fig 10, $k > 1{,}5$ — there is little difference between subtransient and steady-state a.c. and in short-circuit oscillogramms merely the d.c. component will frequently play a substantial role.

8. Negative sequence reactance

In inductor machines, as stated in Para. 2.2, at the quadrature axis no flux linkage exists between armature windings and field-winding. Also, since the damper windings are concentric with the latter, they are not linked with the armature windings. Consequently:

$$X_q = X'_q = X''_q = X_{s1} + X_{aq} \quad (8.1)$$

According to this [11], the negative sequence reactance of heteropolar inductor alternators having no damping turns will be

$$X_2 = \sqrt{X'_d \cdot X_q} \quad (8.2)$$

and if with damper turns provided on the stator

$$X_2 = \sqrt{X_d'' \cdot X_q} \tag{8.3}$$

Reactance of quadrature-axis armature-reaction needed for the calculation of negative sequence reactance can be obtained from Equation (6.4).

9. Single phase short-circuit currents

As is known [8, 10, 11], in the case of line to line single-phase short-circuit of a three-phase synchronous alternator the ratio of transient or subtransient and steady-state a.c.-s is always less than in the case of three-phase short-circuit [11].

With inductor alternators it may happen [1] that $X_q > X_d$. For this reason, and also because of (6.11) $X_d/X_d' \leq 1{,}3$ and by (7.6) $X_d/X_d'' \leq 1{,}44$, and since for (8.1) $X_q = X_q' = X_q''$ the above statement made in the previous paragraph does not always hold true.

For reasons discussed at the conclusion of Para 7 for *single-phase middle-frequency inductor alternators* there can scarcely be found any difference between steady-state and transient, or subtransient short-circuit currents.

In the test-room of the *Ganz* Electrical Works the author conducted sudden short-circuit tests on several single-phase inductor alternators. In the obtained short-circuit oscillograms, in addition to steady-state short-circuit currents, *only d.c. components could be reliably demonstrated.*

10. Graphical method for the determination of air-gap field harmonics

With the known rotor-teeth dimensions and air-gap width the specific permeance curve ($p_{(a)}$) of the variable air-gap can be plotted.

According to rules of harmonic analysis, the value of any of the permeance-harmonics of curve $p_{(a)}$ can be found graphically. It is practical to relate the values so obtained to the same basic permeance values. The best reference base is the specific permeance of the air-gap at a rotor tooth

$$p_{\max} = \frac{\mu_0}{\delta_{\min}} \tag{10.1}$$

With the given rotor tooth shape, the ratios $p_\nu/p_{\max}$ only depend on the dimensional factors δ/t and z/t of rotor-teeth, and are independent of the actual tooth dimensions.

Relative permeance values can be plotted in terms of the latter by a generally valid family of curves. The results obtained for the semicircular rotor slot [7] shown in Fig 2 can be seen on Figs 7, 8 and 9. From these the relative values of permeance-harmonics p_0, p_1 and p_2, firstly needed for the calculations, can be found.

In Fig 10 the factor k of Equation (6.6) is plotted in terms of z/t and δ/t.

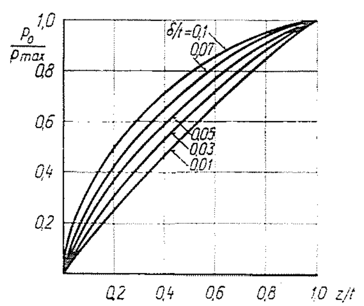

Fig. 7. Relative values of constant component of air-gap permeance

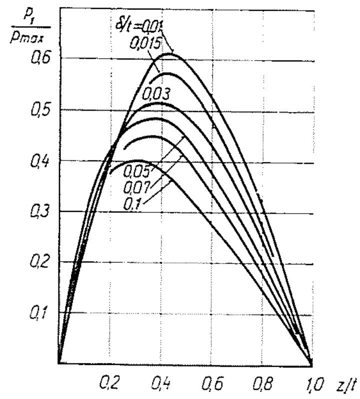

Fig. 8. Relative values of air-gap permeance first harmonic

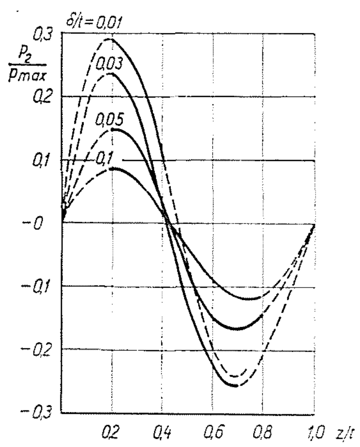

Fig. 9. Relative values of air-gap permeance second harmonic

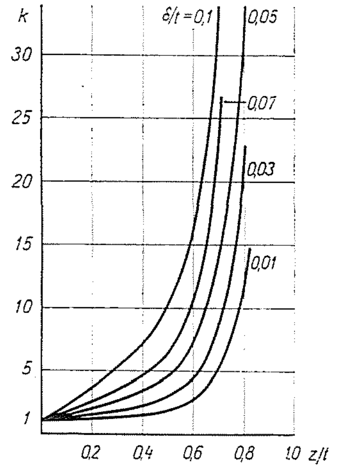

Fig. 10. Varying of factor k in terms of z/t and δ/t

With the aid of these curves numerical values *of all the characteristic electrical parameters of inductor alternators can be found* without having to draw the flux-distribution diagram for a particular case.

11. Numerical example, test results

The author in the following discusses calculated and measured data of a three-phase heteropolar inductor alternator.

Performance data of the alternator tested: 182 kVA, 85 V, 1240 A, $\cos\varphi = 0.9$, three-phase, 3000 r.p.m., 500 cps, with Δ connected armature. No damping circuits are provided.

$$\delta_{\min} = 3 \text{ mm}, \qquad N_r = p = 10$$

$$\tau = 102 \text{ mm}, \qquad t = 204 \text{ mm}, \qquad z = 86 \text{ mm}$$

$$\delta/t = 0.0147 \qquad z/t = 0.42$$

$$N_g = 4 \qquad N = 4 \cdot 24 = 96 \qquad q = 2$$

Pitch of armature slots: 1/120, thus $\varkappa = 0{,}8$

$$w_g/N_g = 95 \text{ turns per pole}$$

$$w = 6 \text{ turns per phase}$$

Maximum air-gap permeance

$$p_{\max} = \frac{1.256}{0.3} = 4.19$$

Relative magnetic permeances:

$$\frac{p_0}{p_{\max}} = 0.51; \qquad \frac{p_1}{p_{\max}} = 0.57; \qquad \frac{p_2}{p_{\max}} = 0.07$$

Leakage permeances of armature and field winding:

$$\sum \frac{\lambda}{q} = 1.64; \quad p_{s1} = 0.565; \quad \sum \lambda_g = 1.5; \quad p_{s2} = 3.35$$

$$\frac{p_{s1}}{p_{\max}} = 0.135; \qquad \frac{p_{s2}}{p_{\max}} = 0.8$$

According to Equation (3.1) the equation of air-gap line of phase voltage is

$$U = 10.9 \cdot I_g$$

For $I_g = 10$ A this gives $U = 109$ V, measured value for this field current is 104 V.

By Equation (6.5) $C = 4.9 \cdot 10^{-2}$ and, by Equation (6.4)

$$\begin{aligned} X_{s1} &= 0.0277\,\Omega \\ X_{ad} &= 0.1115\,\Omega \\ \hline X_d &= 0.1392\,\Omega \end{aligned}$$

$$X_m = 0.0825\,\Omega \qquad X_g = 0.1045\,\Omega$$

Steady-state short-circuit current is from Equation (4.3)

$$I_a = 81.5 \cdot I_g$$

for an excitation $I_g = 10$ A, $I_a = 815$ A against the measured value of 800 A.

From Equation (6.6) and Fig 10, respectively,

$$k = 1.72$$

By Equation (6.4) $\quad X'_{s2} = 0.164\ \Omega$

By Equation (6.1) $\quad X'_d = 0.1136\ \Omega$

and

$$\frac{X_d}{X'_d} = 1.22$$

On the other hand, the sudden short-circuit test made from 93 V resulted in a reactance ratio of

$$\frac{X_d}{X'_d} = 1.16 \sim 1.29$$

In the field current practically no transient phenomena could be observed.

12. Summary

The paper reviews the properties of flux-linkage between armature and field windings by means of investigation of fields generated in the air-gap of three-phase inductor alternators. On this basis the author demonstrates the ratio of synchronous and transient, or subtransient reactances to be much lower in inductor machines than in alternate-pole machines. Consequently, in single-phase inductor machines there is hardly any difference between the transient or subtransient and the steady-state a.c.-s. By drawing flux-distribution diagrams for an air-gap, generally valid curves are obtained from which the air-gap permeance harmonics can be evaluated for each tooth shape. By using these curves the air-gap line of no-load characteristic, short-circuit characteristic and also the synchronous, transient, subtransient and negative sequence reactances can be calculated. The use of the calculation method is illustrated by a numerical example, and calculated and measured values being in good concord, are compared.

13. List of Symbols

α $= \frac{x}{\tau}\pi$ electrical angle measured at the stator circumference
δ air-gap width
$\delta_{\min}$ air-gap width at rotor tooth
Θ magnetomotive force, m. m. f.
$\Theta_{a1\max}$ amplitude of armature m. m. f. fundamental
Θ_g field winding m. m. f.
$\Theta_{g\ddot{u}}$ field winding m. m. f. at no-load
Θ_{gv} field current a. c. component m. m. f. (at sudden short-circuit)
Θ_{ge} field current d. c. component m. m. f. (at sudden short-circuit)
Θ_{av} armature current a. c. component m. m. f. (at sudden short-circuit)
Θ_{ae} armature current d. c. component m. m. f. (at sudden short-circuit)
Ψ flux-linkage
$\sum \frac{\lambda}{q}$ resultant leakage permeance of armature winding per q slots and unit machine length
$\Sigma\lambda_g$ resultant leakage permeance of field winding per unit machine length
μ_0 vacuum permeability
ν order of harmonic

τ	pole pitch
ω	angular velocity
$\varkappa$	slot omission ratio
C	constant term in Equ.-s (6.4) and (6.5)
c	constant term in Equ.-s (4.1), (5.1) and (5.2)
f	frequency (c.p.s.)
I_g	excitation (field) current
I_a	armature current
k	Alper's linkage factor in Equ. (6.2)
l_i	virtual machine length
m_1	phase number of armature winding
N_r	No of rotor teeth $(=p)$
N_g	No of excitation poles
N	No of slots of armature winding per phase
n	speed r.p.m.
p	No of pole pairs $(=N_r)$
p	$=\mu_0/\delta$ specific magnetic permeance of air-gap
p_ν	ν-th harmonic of air-gap specific magnetic permeance
ξ_1	reduction factor of armature winding fundamental
$p_{\max}$	max. value of air-gap permeance (at rotor tooth)
p_{s1}	equivalent leakage permeance of armature winding
p_{s2}	equivalent leakage permeance of excitation winding
q	No. of slots per pole and phase
t	rotor slot pitch; time
U	phase voltage
w	in series connected armature turns per phase
w_g	total series-connected turns of excitation winding
X_{ad}	reactance of direct-axis armature reaction
X_{aq}	reactance of quadrature-axis armature reaction
X_{s1}	armature leakage reactance
X_{s2}'	field winding leakage reactance reduced to armature
X_d	direct-axis synchronous reactance
X_q	quadrature-axis synchronous reactance
X_d'	direct-axis transient reactance
X_q'	quadrature-axis transient reactance
X_d''	direct-axis subtransient reactance
X_q''	quadrature-axis subtransient reactance
X_2	negative sequence reactance
X_m	reactance of mutual inductance
X_g	excitation winding air-gap field reactance
X_{cs}'	damping turn leakage reactance reduced to armature
x	distance measured at stator-bore circumference
z	rotor tooth width

14. References

1. ALPER, N. J.: Basic Problems on the Theory of Inductor Alternators (in Russian) Vestnik Elektropromyshlen. p. 27—33 (1961).
2. WALKER, J. H.: The Theory of Inductor Alternator, Journal of the IEE, p. 227—241 (1942).
3. ASZTALOS, P.: Middle Frequency Alternators (in Hungarian), Elektrotechnika, pp. 166—176, 208—214 (1953).
4. DOHERTY, R. E.—NICKLE, C. A.: Synchronous Machines I. AIEE Transactions, p. 912—947 (1926).
5. HÖRCHER, F.: Asynchronous Operation of Synchronous Motors (in Hungarian), Academical study, Budapest 1953. M. S.
6. WIESEMAN, R. W.: Graphical Determination of Magnetic Fields, Journal AIEE, 430—437 (1927).
7. ASZTALOS, P.: Design Problems of Inductor Alternators (in Hungarian), Elektrotechnika 340—349 (1955).

8. Kovács, K. P.—Rácz, I.: Transient Phenomena in A. C. Machines (in Hungarian). Budapest 1954.
9. Tuschák, R.: Design of the Starting Cage of Synchronous Motors (in Hungarian), Dissertation, Budapest 1962.
10. Geszti, O. P., Kovács, K. P., Vajta, M.: Symmetrical Components (in Hungarian). Budapest. 1959.
11. Kovács, K. P.—Rácz, I.: Transiente Vorgänge in Wechselstrom-Maschinen, Budapest, 1959.
12. Lehmann, Th.: Graphische Methode zur Bestimmung des Kraftlinienverlaufes in der Luft, ETZ 995, 1019 (1909).

Péter Asztalos, Budapest, XI. Holdvilág u. 4. Hungary